



## MHD Natural Convection Flow of Casson Ferrofluid at Lower Stagnation Point on a Horizontal Circular Cylinder

Muhammad Khairul Anuar Mohamed<sup>1,\*</sup>, Huei Ruey Ong<sup>2</sup>, Siti Khuzaimah Soid<sup>3</sup>, Hamzeh Taha Alkassabeh<sup>4</sup>

<sup>1</sup> Centre for Mathematical Sciences, University Malaysia Pahang Al-Sultan Abdullah, Lebu Persiaran Tun Khalil Yaakob, 26300 Kuantan, Malaysia

<sup>2</sup> Faculty of Engineering Technology, DRB-HICOM University of Automotive Malaysia, Peramu Jaya Industrial Area, 26607 Pekan, Malaysia

<sup>3</sup> School of Mathematical Sciences, College of Computing, Informatics, and Mathematics, Universiti Teknologi MARA, Malaysia

<sup>4</sup> Department of Mathematics, Faculty of Science, Ajloun National University, P.O. Box 43, Ajloun 26810, Jordan

### ARTICLE INFO

#### Article history:

Received 28 July 2024

Received in revised form 25 August 2024

Accepted 22 September 2024

Available online 30 October 2024

#### Keywords:

Casson; Ferrofluid; Horizontal circular cylinder; Keller-box; Stagnation

### ABSTRACT

This study extends the mathematical model of MHD free convection flow on horizontal circular cylinder, with considering the Casson ferrofluid, specific to a stagnation region case. The set of non-linear partial differential equations that governed the model is first transformed to a simpler set of equations using the non-similar transformation. This set of equations then reduced to ordinary partial equations which reflects to the case of stagnation region and solved numerically using the implicit finite difference method known as the Keller-box method. Blood and magnetite are taken as the based-fluid and the ferroparticles for the Casson ferrofluid, respectively. From the numerical study, it was found that the Casson ferrofluid with the same Prandtl values had higher thermal and velocity boundary layer thicknesses compared to a Newtonian ferrofluid. The increase of Casson parameter reduced the thermal boundary layer thickness which physically enhanced the Nusselt number.

## 1. Introduction

The flow of fluid containing magnetic nanoparticles known as ferroparticles plays an important role in medicine. Induced by the magnetic field, this fluid is known as ferrofluid. Ferrofluid contains engineered colloidal suspensions of magnetic nanoparticles like cobalt, magnetite and ferrite scattered based fluid like water and oil. Ferrofluid originally was invented by NASA as liquid rocket fuel at no gravity situation [1]. Magnetic field is applied to direct the liquid rocket fuel containing the ferroparticles to a rocket combustion chamber. Ferrofluid are employed in medics as cancer treatment, reducing bleeding in severe injuries, magnetic resonance imaging and other diagnostic tests [2]. In the industrial segment, the ferrofluid is applied in electronic devices cooling systems for example in hi-fi speakers and computer hard-disc. Ferrofluid is found in the transportation segment as heat controlling agents in an electric motors [3].

\* Corresponding author.

E-mail address: [mkhairulanuar@umpsa.edu.my](mailto:mkhairulanuar@umpsa.edu.my) (Muhammad Khairul Anuar Mohamed)

Some of the industrial fluid employed shows different characteristics compared to a Newtonian fluid like water. This non-Newtonian characteristic usually couldn't be presented by classical Navier-Stokes equations [4]. Therefore, some modifications to the Navier-Stokes equations are proposed in many previous studies [5]. The Casson fluid model is one of the non-Newtonian models introduced to characterize the fluid elastic solid behavior. It is well known that Casson fluid is a shear-thinning liquid that is assumed to have an infinite viscosity at zero rates of shear, yield stress below which no flow occurs, and a zero viscosity at an infinite rate of shear [6]. Physically, the fluid behaves like a solid when the shear stress is less than the yield stress. As shear stress is applied is greater than the yield stress, then the fluid starts to move. From this character, it is known that tomato sauce, honey, concentrated fluid, jelly as well as human blood is an example of Casson fluid. According to Khalid *et al.*, [7], Casson model is identified as the most preferred rheological model for describing human blood flow. Recent study on Casson ferrofluid included the works by Jalili *et al.*, [8], Awais *et al.*, [9], Das and Dey [10] and Leelavathi *et al.*, [11] who investigated radiative heat transfer with magnetic field of non-Newtonian Casson fluid past a shrinking surface and stagnation point flow over an inclined porous surface with enthalpy change.

Considering the study of the convective flow towards circular cylinder, the free and mixed convection boundary layer on an isothermal horizontal cylinder have been studied by Merkin [12,13]. This is the first study to obtain the exact solution. Merkin and Pop [14] updated this topic with constant heat flux (CHF). Since then, many related studies have been made by the researchers includes extending the scope to a non-Newtonian fluid, external effect as well as the boundary conditions for example the study on free and mixed convection flow over a horizontal circular cylinder in hybrid nanofluid, Williamson nanofluid and second grade nanofluid with viscous dissipation, thermal radiation and chemical reaction effects [15-20].

In this study, the natural convection flow of ferrofluid considering the Casson model is numerically investigated. Considering the flow towards a lower stagnation point on a horizontal circular cylinder, such studies have never been done before via numerical or experimental analysis. The classical Navier-Stokes equations are extended considering the Casson model, ferroparticle volume fraction and magnetic effects. The non-similarity transformation is applied to eliminate as much as possible a dependent variable. The study is limited to a case at a lower stagnation point, thus the transformed partial differential equations obtained are reduced to ordinary differential equation and solved numerically using Keller-box method. This study aims to investigate; what is the effects of magnetic field and the ferroparticles on a fluid flow; and what is the effects of the Casson parameter in heat transfer. It is worth mentioning here that, results discussed in this study are new.

## 2. Mathematical Formulation

Consider the horizontal circular cylinder with radius  $a$ , heated to a constant temperature  $T_w$  and embedded in a blood-based Casson ferrofluid with ambient temperature  $T_\infty$ . The orthogonal coordinates of  $x$  and  $y$  are measured along the cylinder surface, starting with the lower stagnation point ( $x = 0$ ), and normal to it, respectively. The physical model of the coordinate system is shown in Figure 1. Further, a uniform magnetic field of strength  $B_0$  is assumed to be applied normal on the cylinder surface. The magnetic Reynolds number is assumed to be small, and thus the induced magnetic field is negligible. The dimensional governing equations of the convective heat and the fluid flow are represented by [21-23].

$$\frac{\partial u}{\partial x} + \frac{\partial v}{\partial y} = 0, \quad (1)$$

$$u \frac{\partial u}{\partial x} + v \frac{\partial u}{\partial y} = \nu_{ff} \left( 1 + \frac{1}{\beta} \right) \frac{\partial^2 u}{\partial y^2} + \beta_{ff} g (T - T_\infty) \sin \frac{x}{a} - \frac{\sigma_{ff} B_o^2(x)}{\rho_{ff}} u, \quad (2)$$

$$u \frac{\partial T}{\partial x} + v \frac{\partial T}{\partial y} = \frac{k_{ff}}{(\rho C_p)_{ff}} \frac{\partial^2 T}{\partial y^2}, \quad (3)$$

subject to the boundary conditions

$$\begin{aligned} u(x, 0) = v(x, 0) = 0, \quad T(x, 0) = T_w, \\ u(x, \infty) \rightarrow 0, \quad T(x, \infty) \rightarrow T_\infty, \end{aligned} \quad (4)$$

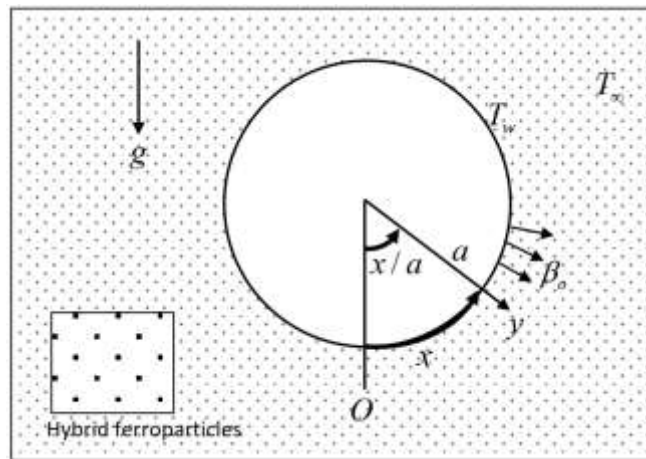


Fig. 1. Physical model of the horizontal circular cylinder

where  $u$  and  $v$  are the velocity components along the  $x$  and  $y$  axes, respectively.  $T$  is taken as temperature of the fluid inside the boundary layer while  $\beta$  and  $g$  is the Casson parameter and gravity acceleration, respectively. Furthermore,  $\nu_{ff}$ ,  $\beta_{ff}$ ,  $\sigma_{ff}$ ,  $\rho_{ff}$ ,  $k_{ff}$  and  $(\rho C_p)_{ff}$  is taken as the Casson ferrofluid's kinematic viscosity, the thermal expansion, the electrical conductivity, density, the thermal conductivity and the heat capacity respectively. Other properties related to a Casson ferrofluid, it based fluid (blood) and the ferroparticles are denoted with subscript  $_{ff,f}$  and  $_s$  respectively as follows [24]:

$$\begin{aligned} \nu_{ff} = \mu_{ff} / \rho_{ff}, \quad \rho_{ff} = (1-\phi)\rho_f + \phi\rho_s, \quad \alpha_{ff} = k_{ff} / (\rho C_p)_{ff}, \quad \mu_{ff} = \mu_f / (1-\phi)^{2.5}, \\ (\rho C_p)_{ff} = (1-\phi)(\rho C_p)_f + \phi(\rho C_p)_s, \quad (\rho\beta)_{ff} = (1-\phi)(\rho\beta)_f + \phi(\rho\beta)_s, \\ \frac{k_{ff}}{k_f} = \frac{k_s + 2k_f - 2\phi(k_f - k_s)}{k_s + 2k_f + \phi(k_f - k_s)}. \end{aligned} \quad (5)$$

where  $\phi$  are the ferroparticle volume fraction. To solve the governing Eqs. (1)-(3), the equations must first be reduced to a non-dimensional equation. The set of non-dimensional variables are shown as follows:

$$X = \frac{x}{a}, \quad Y = Gr^{1/4} \frac{y}{a}, \quad U = \frac{a}{v_f} Gr^{-1/2} u, \quad V = \frac{a}{v_f} Gr^{-1/4} v, \quad \theta(\eta) = \frac{T - T_\infty}{T_w - T_\infty}. \quad (6)$$

where  $\theta$  are the rescaled dimensionless temperature of the fluid and  $Gr = \frac{g \beta_f (T_w - T_\infty) a^3}{v_f^2}$  is the Grashof number. Substitute the non-dimensional variables in Eq. (6) into Eqs. (1)-(3) becomes

$$\frac{\partial U}{\partial X} + \frac{\partial V}{\partial Y} = 0, \quad (7)$$

$$U \frac{\partial U}{\partial X} + V \frac{\partial U}{\partial Y} = \frac{v_{ff}}{v_f} \left( 1 + \frac{1}{\beta} \right) \frac{\partial^2 U}{\partial Y^2} + \frac{(\rho\beta)_{ff}}{\rho_{ff} \beta_f} \theta \sin X - MU, \quad (8)$$

$$U \frac{\partial \theta}{\partial X} + V \frac{\partial \theta}{\partial Y} = \frac{k_{ff} / k_f}{(1-\phi) + \phi(\rho C_p)_s / (\rho C_p)_f} \frac{1}{Pr} \frac{\partial^2 \theta}{\partial Y^2}, \quad (9)$$

subject to boundary conditions

$$\begin{aligned} U(X, 0) = 0, \quad V(X, 0) = 0, \quad \theta(X, 0) = 1, \\ U(X, \infty) \rightarrow 0, \quad \theta(X, \infty) \rightarrow 0. \end{aligned} \quad (10)$$

The magnetic parameter and the Prandtl number are defined as  $M = \frac{a^2 \sigma_{ff} B_o^2(x)}{v_f \rho_{ff} Gr^{1/2}}$  and

$$Pr = \frac{v_f (\rho C_p)_f}{k_f}, \quad \text{respectively.} \quad \text{By definition,} \quad \frac{v_{ff}}{v_f} = \frac{1}{(1-\phi)^{2.5} [1 - \phi + (\phi \rho_s) / (\rho_f)]} \quad \text{and}$$

$$\frac{(\rho\beta)_{ff}}{\rho_{ff} \beta_f} = \frac{(1-\phi)\rho_f + \phi(\rho\beta)_s / \beta_f}{(1-\phi)\rho_f + \phi\rho_s}.$$

The non-dimensional Eqs. (7)-(10) obtained have many dependent variables. Reducing the number of dependent variables may ease the solving procedure. Thus, let

$$\psi = Xf(X, Y), \quad \theta = \theta(X, Y), \quad (11)$$

where  $\psi$  is the stream function defined as  $u = \frac{\partial \psi}{\partial Y}$  and  $v = -\frac{\partial \psi}{\partial X}$  which identically satisfies Eq. (7).

By substituting the Eq. (11) into Eqs. (8) and (9), the following transformed partial differential equations are obtained:

$$\frac{\nu_{ff}}{\nu_f} \left( 1 + \frac{1}{\beta} \right) \frac{\partial^3 f}{\partial Y^3} + f \frac{\partial^2 f}{\partial Y^2} - \left( \frac{\partial f}{\partial Y} \right)^2 + \frac{(\rho\beta)_{ff}}{\rho_{ff}\beta_f} \frac{\sin X}{X} \theta - M \frac{\partial f}{\partial Y} = X \left( \frac{\partial f}{\partial Y} \frac{\partial^2 f}{\partial X \partial Y} - \frac{\partial f}{\partial X} \frac{\partial^2 f}{\partial Y^2} \right), \quad (12)$$

$$\frac{k_{ff}/k_f}{(1-\varphi) + \varphi(\rho C_p)_s / (\rho C_p)_f} \frac{1}{Pr} \frac{\partial^2 \theta}{\partial Y^2} + f \frac{\partial \theta}{\partial Y} = X \left( \frac{\partial f}{\partial Y} \frac{\partial \theta}{\partial X} - \frac{\partial f}{\partial X} \frac{\partial \theta}{\partial Y} \right). \quad (13)$$

with boundary conditions

$$f(X, 0) = 0, \quad \frac{\partial f}{\partial Y}(X, 0) = 0, \quad \theta(X, 0) = 1, \quad (14)$$

$$\frac{\partial f}{\partial Y}(X, \infty) \rightarrow 0, \quad \theta(X, \infty) \rightarrow 0.$$

At lower stagnation region ( $X = 0$ ), the transformed Eqs. (12) and (13) are reduced to a set of ordinary differential equations

$$\frac{\nu_{ff}}{\nu_f} \left( 1 + \frac{1}{\beta} \right) f''' + ff'' - f'^2 + \frac{(\rho\beta)_{ff}}{\rho_{ff}\beta_f} \theta - Mf' = 0, \quad (15)$$

$$\frac{k_{ff}/k_f}{(1-\varphi) + \varphi(\rho C_p)_s / (\rho C_p)_f} \frac{1}{Pr} \theta'' + f\theta' = 0. \quad (16)$$

Note that ' is derivatives with respect to  $Y$ . The boundary conditions become

$$f(0, 0) = 0, \quad f'(0, 0) = 0, \quad \theta(0, 0) = 1, \quad (17)$$

$$f'(0, \infty) \rightarrow 0, \quad \theta(0, \infty) \rightarrow 0.$$

The physical quantities of interest is the local Nusselt number  $Nu_x$  given by [25]

$$Nu_x = \frac{aq_w}{k_f(T_w - T_\infty)}, \quad (18)$$

and reduced to

$$Nu_x Gr^{-1/4} = -\frac{k_{ff}}{k_f} \theta'(0, 0). \quad (19)$$

### 3. Numerical Method and Computations

The transformed ordinary differential Eqs. (15)-(16) subjected to the boundary conditions (17) was solved numerically by using the Keller-box method. It is the finite difference method in conjunction with the Newton's method for the linearization. Keller-box method is known for its unconditionally stable thus provided precise numerical results. It is also suitable for solving non-linear the ordinary differential equation as well as the partial differential equations at any order. As discussed in the books by Na [26], Cebeci and Cousteix [27] and Mohamed [28], the Keller-box consists of 4 steps which starts with reducing the Eqs. (15)-(16) to a first-order system. Next, the midpoint of the net rectangle is written by using the central differences. Noticed that the non-linear equations need to be linearize before being solved, thus Newtons method is implemented. The resulting algebraic equations are then written in matrix-vector the form and lastly, being solved by the block tridiagonal elimination technique.

The algorithm of the Keller-box method is coded into a MATLAB software to generate the numerical results and graphs. The algorithm is developed considering the 4 steps of the Keller-box method. The previous publications applying the Keller-box method and MATLAB for computations included the works by Zokri *et al.*, [29], Yasin *et al.*, [30], Zaki *et al.*, [31], Rosli *et al.*, [32-33] and recently by Elfiano *et al.*, [19].

### 4. Results and Discussion

In generating the numerical computation, the boundary layer thickness set between 7 to 12 is sufficient to provide the accurate results. In this study, the numerical solutions are obtained for the reduced Nusselt number  $Nu_x Gr_x^{-1/4}$  for a various values of magnetic parameter  $M$ , Casson parameter  $\beta$  and the ferroparticles volume fraction  $\phi$ . The magnetite  $Fe_3O_4$  and cobalt ferrite  $CoFe_2O_4$  are taken as the ferroparticles for the blood-based Casson ferrofluid. The thermophysical properties of blood and the ferroparticles are shown in Table 1. For results validating purpose, Table 2 shows the comparison for the present results with the previous published. It is clearly shown the efficiency of the Keller-box method applied in this study.

**Table 1**  
 Thermophysical properties of blood and ferroparticles [7]

Physical Properties	Blood ( $f$ )	$Fe_3O_4$	$CoFe_2O_4$
$\rho$ (kg/m <sup>3</sup> )	1053	5180	4907
$C_p$ (J/kg·K)	3594	670	700
$k$ (W/m·K)	0.492	9.7	3.7

**Table 2**

Comparison values of  $Nu_x Gr_x^{-1/4}$  from Eqs. (12)-(13) with previous studies for various values of  $X$  when  $Pr=1$  and  $M=0$ .

$X$	$\phi=0$ and $\beta \rightarrow \infty$		$\phi=0.1 (Fe_3O_4)$ and $\beta=0.5$	
	Merkin [12]	Azim [21]	Present	Present
0	0.4214	0.4216	0.4213	0.4127
$\pi/6$	0.4161	0.4163	0.4162	0.4062
$\pi/3$	0.4007	0.4006	0.4006	0.3907
$\pi/2$	0.3745	0.3742	0.3742	0.3647
$2\pi/3$	0.3364	0.3356	0.3358	0.3264
$5\pi/6$	0.2825	0.2811	0.2820	0.2719
$\pi$	0.1945	0.1912	0.1936	0.1800

Figure 2 to 5 are plotted considering the Ferrite  $Fe_3O_4$  as the ferroparticles. The temperature profiles  $\theta(Y)$  and the velocity profiles  $f'(Y)$  for various values of Casson parameter  $\beta$  are shown in Figures 2 and 3, respectively. It is found that the increase of  $\beta$  reduced both thermal and velocity boundary layer thicknesses. The reduction in thermal boundary layer thicknesses physically denoted to an increase in temperature gradient thus led to the enhanced of the  $Nu_x Gr_x^{-1/4}$ . Further, from Figure 3, it is found that the fluid velocity increases as  $\beta$  increases. Note that as  $\beta \rightarrow \infty$ , the Casson effect is neglected, and the fluid acted as the Newtonian fluid. This gave an idea that the Newtonian fluid with the same values of Pr has lower thermal and velocity boundary layer thicknesses compared to a Casson fluid.

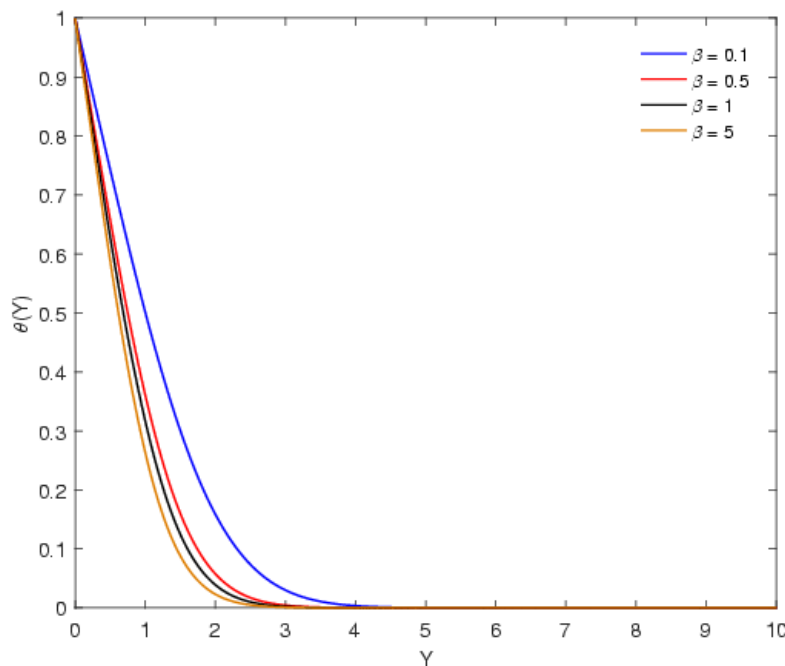


**Fig. 2.** Temperature profiles  $\theta(Y)$  for different various of  $\beta$

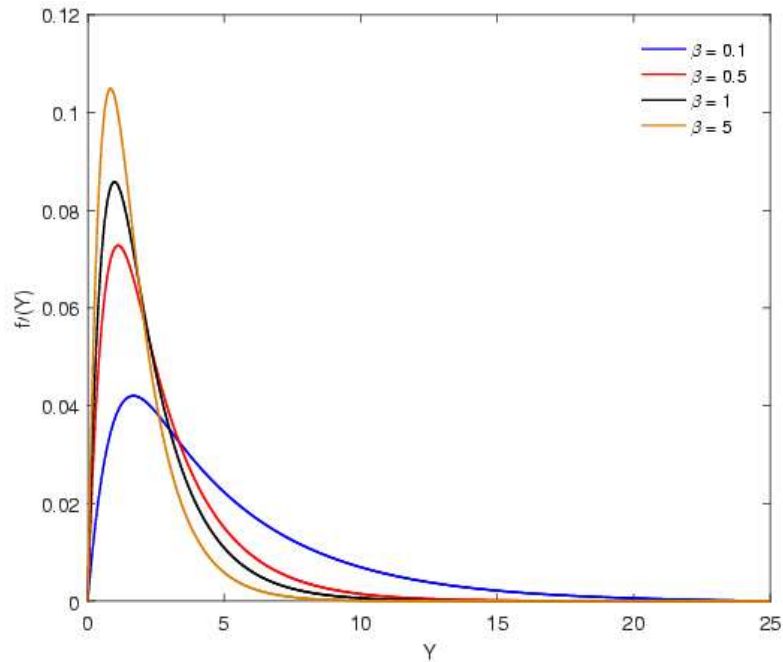
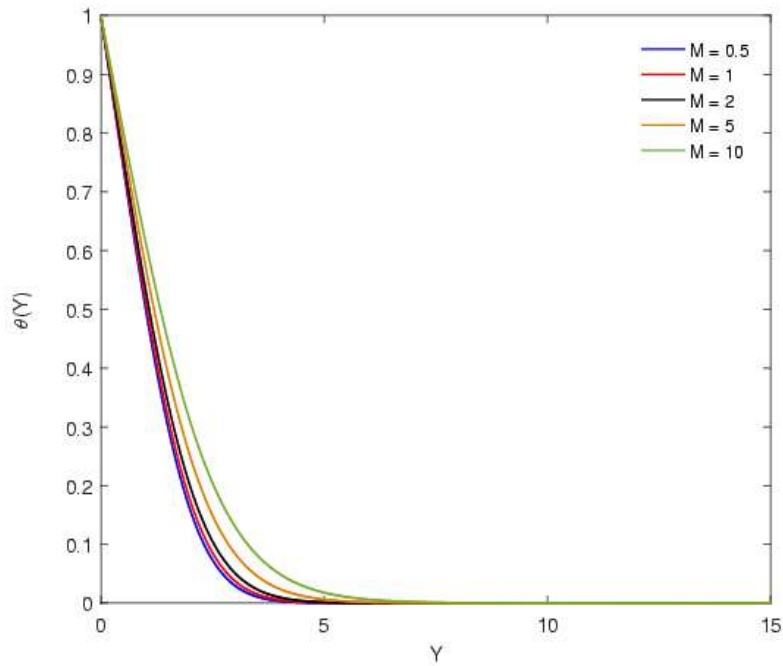


Fig. 3. Velocity profiles  $f'(Y)$  for different various of  $\beta$

In considering the magnetic effects on the fluid flow and the heat transfer, the temperature profiles  $\theta(Y)$  and the velocity profiles  $f'(Y)$  for various values of magnetic parameter  $M$  are illustrated in Figures 4 and 5. From this figure, it is observed that the increase of  $M$  results to the increase in the thermal boundary layer thickness but reduced the fluid velocity and its boundary layer thicknesses. In Figure 5, the increase of  $M$  led to the increase of the Lorentz forces, thus hold the Casson ferrofluid particles which slow down the fluid velocity. The reduction of velocity proportionally reflects to the reduction of the velocity boundary layer thickness.

The increase in  $M$  has tied the ferroparticle in fluid thus enhanced fluid conduction abilities. As shown in Figure 4, it is concluded that the thickening in thermal boundary layer as  $M$  increases physically refers to the reduction in  $Nu_x Gr_x^{-1/4}$ , thus reducing the convective heat transfer capabilities in the fluid flow. It is realistic since the reducing of convection refers to the increase of conduction abilities in fluid flow.





**Fig. 4.** Temperature profiles  $\theta(Y)$  for different various of  $M$

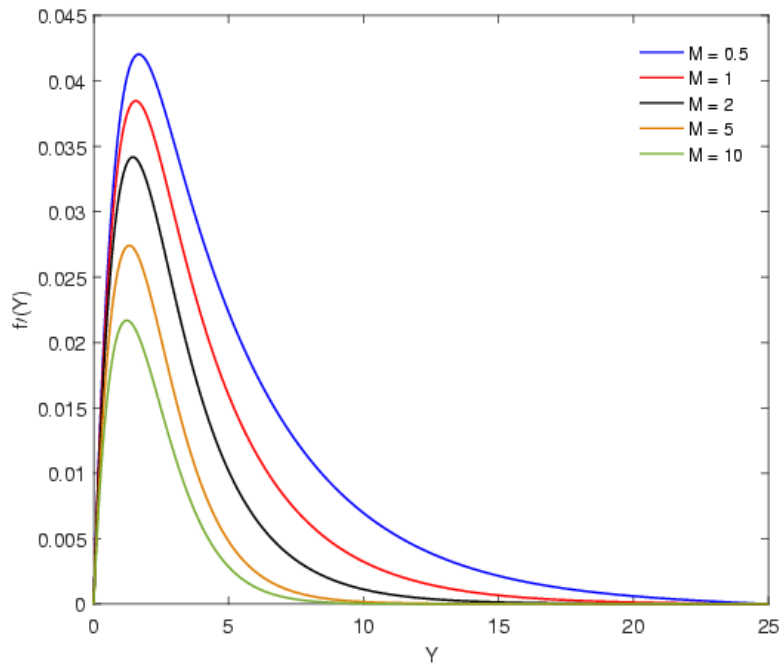


**Fig. 5.** Velocity profiles  $f'(Y)$  for different various of  $M$

Next, the variation of  $Nu_x Gr_x^{-1/4}$  against  $\beta$  and  $M$  are plotted in Figures 6 and 7, respectively. Considering 3 different particles and its volume fractions, the variation of  $Nu_x Gr_x^{-1/4}$  are plotted regards to 10%  $Fe_3O_4$ , 15%  $Fe_3O_4$  and 10%  $CoFe_2O_4$  blood-based Casson ferrofluid. From Figure 6, it is shows that the increase of  $\beta$  in range of  $\beta < 1$  had drastically enhanced the values of  $Nu_x Gr_x^{-1/4}$ . As  $\beta > 1$ , the increase of  $\beta$  gave small increment on  $Nu_x Gr_x^{-1/4}$ . Meanwhile, the opposite trend occur on  $M$  as agreed in Figure 4. The increase of  $M$  reduced the values of  $Nu_x Gr_x^{-1/4}$ . Noticed that,

as ferroparticle volume fraction  $\phi$  increases, the  $Nu_x Gr_x^{-1/4}$  also increases. The increase amount of ferroparticles dissipate heat more efficiently thus contribute better to heat convection abilities.  $Fe_3O_4$  has higher thermal conductivity than  $CoFe_2O_4$ , as shown in Table 1. This results to a high in  $Nu_x Gr_x^{-1/4}$  variations for the blood-based Casson ferrofluid with 10%  $Fe_3O_4$   $Nu_x Gr_x^{-1/4}$  compared to the blood-based Casson ferrofluid with 10%  $CoFe_2O_4$ .

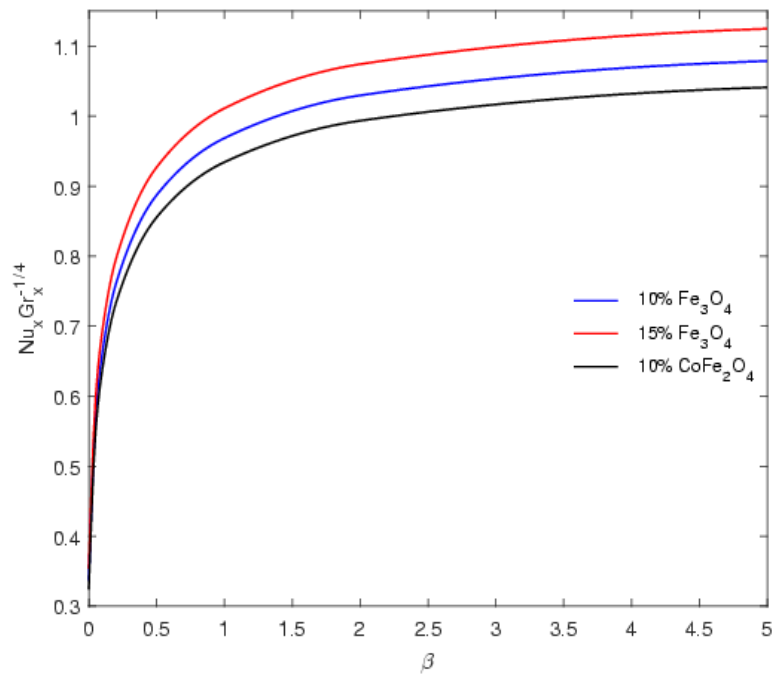


Fig. 6. Variation values of  $Nu_x Gr_x^{-1/4}$  for different various of  $\beta$

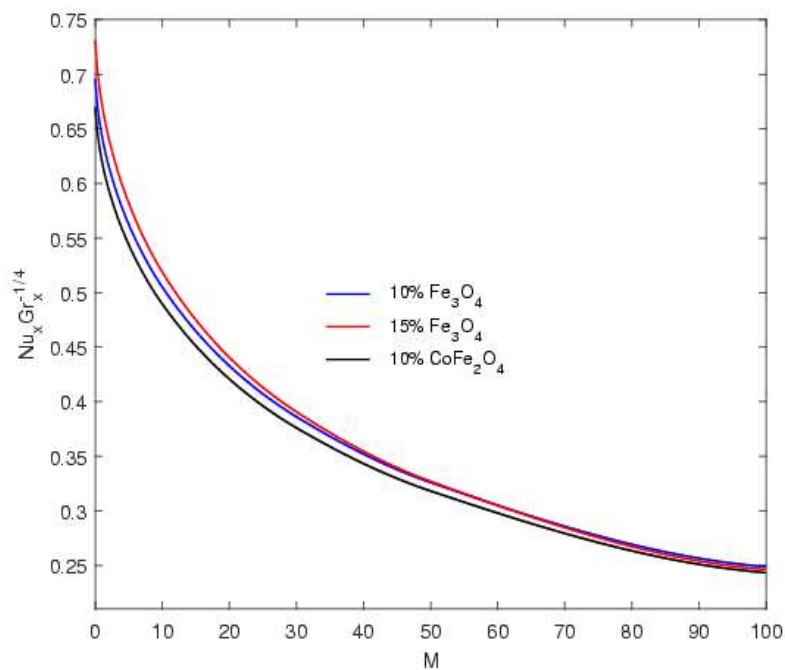


Fig. 7. Variation values of  $Nu_x Gr_x^{-1/4}$  for different various of  $M$

## 5. Conclusion

This study has numerically solved the natural convection flow of a Casson ferrofluid at a lower stagnation point of a horizontal circular cylinder. The effects of ferroparticles in a Casson fluid is the key novelty in this research. It is shown that the Keller-box method used is sufficient to provide precise results and generate the solutions. In summary, it is concluded that the increase of Casson parameter reduced both thermal and velocity boundary layer thicknesses which physically enhanced the Nusselt number. It is also observed that the Newtonian fluid with the same Pr had lower thermal and velocity boundary layer thicknesses compared to a Casson fluid. Furthermore, the increase of  $M$  results to the increase in thermal boundary layer thickness but reducing the Nusselt number and reduced the fluid velocity and its boundary layer thickness. Results obtained in this research provided an early idea on fluid parameters characteristics that will helps the researchers in developing the heat exchanger or cooling devices related to non-Newtonian ferrofluid.

## Acknowledgement

Authors are grateful to acknowledge the Universiti Malaysia Pahang Al-Sultan Abdullah for providing the financial support under research grant no. RDU220388.

## References

- [1] Stephen, Papell Solomon. "Low viscosity magnetic fluid obtained by the colloidal suspension of magnetic particles." U.S. Patent 3,215,572, issued November 2, 1965.
- [2] Rashad, A. M. "Impact of anisotropic slip on transient three-dimensional MHD flow of ferrofluid over an inclined radiate stretching surface." *Journal of the Egyptian Mathematical Society* 25, no. 2 (2017): 230-237.
- [3] Zeeshan, A., A. Majeed, and R. Ellahi. "Effect of magnetic dipole on viscous ferro-fluid past a stretching surface with thermal radiation." *Journal of Molecular liquids* 215 (2016): 549-554.
- [4] Mukhopadhyay, Swati, Prativa Ranjan De, Krishnendu Bhattacharyya, and G. C. Layek. "Casson fluid flow over an unsteady stretching surface." *Ain Shams Engineering Journal* 4, no. 4 (2013): 933-938. <https://doi.org/10.1016/j.asej.2013.04.004>
- [5] Makanda, Gilbert, Sachin Shaw, and Precious Sibanda. "Effects of radiation on MHD free convection of a Casson fluid from a horizontal circular cylinder with partial slip in non-Darcy porous medium with viscous dissipation." *Boundary Value Problems* 2015 (2015): 1-14. <https://doi.org/10.1186/s13661-015-0333-5>
- [6] Pramanik, S. "Casson fluid flow and heat transfer past an exponentially porous stretching surface in presence of thermal radiation." *Ain shams engineering journal* 5, no. 1 (2014): 205-212. <https://doi.org/10.1016/j.asej.2013.05.003>
- [7] Khalid, Asma, Ilyas Khan, Arshad Khan, Sharidan Shafie, and I. Tlili. "Case study of MHD blood flow in a porous medium with CNTS and thermal analysis." *Case studies in thermal engineering* 12 (2018): 374-380.
- [8] Jalili, Payam, Ali Ahmadi Azar, Bahram Jalili, and Davood Domiri Ganji. "Study of nonlinear radiative heat transfer with magnetic field for non-Newtonian Casson fluid flow in a porous medium." *Results in Physics* 48 (2023): 106371. <https://doi.org/10.1016/j.rinp.2023.106371>
- [9] Awais, Muhammad, T. Salahuddin, and Shah Muhammad. "Evaluating the thermo-physical characteristics of non-Newtonian Casson fluid with enthalpy change." *Thermal Science and Engineering Progress* 42 (2023): 101948. <https://doi.org/10.1016/j.tsep.2023.101948>
- [10] Das, Rajesh Kumar, and Debasish Dey. "Casson Fluid Flow Past a Shrinking Surface with Heat and Mass Transfers." *East European Journal of Physics* 1 (2024): 243-249. <https://doi.org/10.26565/2312-4334-2024-1-20>
- [11] Leelavathi, R., Seethamahalakshmi Vyakaranam, T. S. Rao, Venkata Ramana Reddy Gurrampati, and Abayomi Samuel Oke. "MHD Casson Fluid Flow in Stagnation-Point over an Inclined Porous Surface." *CFD Letters* 16, no. 4 (2024): 69-84. <https://doi.org/10.37934/cfdl.16.4.6984>
- [12] Merkin, John H. "Free convection boundary layer on an isothermal horizontal cylinder." *American Society of Mechanical Engineers and American Institute of Chemical Engineers* (1976).
- [13] Merkin, J. H. "Mixed convection from a horizontal circular cylinder." *International Journal of Heat and Mass Transfer* 20, (1977): 73-77. [http://dx.doi.org/10.1016/0017-9310\(77\)90086-2](http://dx.doi.org/10.1016/0017-9310(77)90086-2)
- [14] Merkin, J. H., Pop, I. "A note on the free convection boundary layer on a horizontal circular cylinder with constant heat flux." *Wärme-und Stoffübertragung* 22, (1988): 79-81. <https://doi.org/10.1007/bf01001575>

- [15] Ashraf, Muhammad, and Zia Ullah. "Effects of variable density on oscillatory flow around a non-conducting horizontal circular cylinder." *AIP Advances* 10, no. 1 (2020). <http://dx.doi.org/10.1063/1.5127967>
- [16] Mohamed, Muhammad Khairul Anuar, Mohd Zuki Salleh, Fadhilah Che Jamil, and Ong Huei. "Free convection boundary layer flow over a horizontal circular cylinder in Al<sub>2</sub>O<sub>3</sub>-Ag/water hybrid nanofluid with viscous dissipation." *Malaysian Journal of Fundamental and Applied Sciences* 17, no. 1 (2021): 20-25. <https://doi.org/10.11113/mjfas.v17n1.1964>
- [17] Zokri, Syazwani Mohd, Nur Syamilah Arifin, Zanariah Mohd Yusof, Nursyazni Mohd Sukri, Abdul Rahman Mohd Kasim, Nur Atikah Salahudin, and Mohd Zuki Salleh. "Carboxymethyl cellulose based second grade nanofluid around a horizontal circular cylinder." *CFD Letters* 14, no. 11 (2022): 119-128. <https://doi.org/10.37934/cfdl.14.11.119128>
- [18] Rao, Shiva, and Paramananda Deka. "A numerical study on unsteady MHD Williamson nanofluid flow past a permeable moving cylinder in the presence of thermal radiation and chemical reaction." *Biointerface Research in Applied Chemistry* 13, no. 5 (2023): 436.
- [19] Elfiano, Eddy, Nik Mohd Izual Nik Ibrahim, and Muhammad Khairul Anuar Mohamed. "Mixed Convection Boundary Layer Flow over a Horizontal Circular Cylinder in Al<sub>2</sub>O<sub>3</sub>-Ag/Water Hybrid Nanofluid with Viscous Dissipation." *CFD Letters* 16, no. 4 (2024): 98-110. <https://doi.org/10.37934/cfdl.16.4.98110>
- [20] Ullah, Zia, Muhammad Ashraf, Ioannis E. Sarris, and Theodoros E. Karakasidis. "The impact of reduced gravity on oscillatory mixed convective heat transfer around a non-conducting heated circular cylinder." *Applied Sciences* 12, no. 10 (2022): 5081.
- [21] Azim, N. H. M. A. "Effects of viscous dissipation and heat generation on MHD conjugate free convection flow from an isothermal horizontal circular cylinder." *SOP Transactions on Applied Physics* 1, no. 3 (2014): 1-11.
- [22] Mohamed, Muhammad Khairul Anuar, Norhafizah Md Sarif, Abdul Rahman Mohd Kasim, N. A. Z. M. Noar, Mohd Zuki Salleh, and Anuar Ishak. "Effects of viscous dissipation on free convection boundary layer flow towards a horizontal circular cylinder." *ARPJ Journal of Engineering and Applied Sciences* 11, no. 11 (2016): 7258-7263.
- [23] Ramli, Norshafira, Syakila Ahmad, and Ioan Pop. "Slip effects on MHD flow and heat transfer of ferrofluids over a moving flat plate." In *AIP Conference Proceedings*, vol. 1870, no. 1. AIP Publishing, 2017. <https://doi.org/10.1063/1.4995847>
- [24] Mohamed, Muhammad Khairul Anuar, Nurul Ainn Ismail, Norhamizah Hashim, Norlianah Mohd Shah, and Mohd Zuki Salleh. "MHD slip flow and heat transfer on stagnation point of a magnetite (Fe<sub>3</sub>O<sub>4</sub>) ferrofluid towards a stretching sheet with Newtonian heating." *CFD Letters* 11, no. 1 (2019): 17-27.
- [25] Tham, Leony, Roslinda Nazar, and Ioan Pop. "Mixed convection boundary layer flow from a horizontal circular cylinder in a nanofluid." *International Journal of Numerical Methods for Heat & Fluid Flow* 22, no. 5 (2012): 576-606. <https://doi.org/10.1108/09615531211231253>
- [26] Na, Tsung Yen, ed. *Computational methods in engineering boundary value problems*. Academic press, 1980.
- [27] Cousteix, T. Cebeci J., and J. Cebeci. "Modeling and computation of boundary-layer flows." *Berlin, Germany: Springer* (2005). <https://doi.org/10.1007/3-540-27624-6>
- [28] Mohamed, M. K. A. "Keller-box method: Partial differential equations in boundary layer flow of nanofluid." *DRB-HICOM University Publisher, Pekan* (2018).
- [29] Zokri, Syazwani Mohd, Nur Syamilah Arifin, Muhammad Khairul Anuar Mohamed, Abdul Rahman Mohd Kasim, Nurul Farahain Mohammad, and Mohd Zuki Salleh. "Influence of viscous dissipation on the flow and heat transfer of a Jeffrey fluid towards horizontal circular cylinder with free convection: A numerical study." *Malaysian Journal of Fundamental and Applied Sciences* 14, no. 1 (2018): 40-47.
- [30] Yasin, Siti Hanani Mat, Muhammad Khairul Anuar Mohamed, Zulkhibri Ismail, Basuki Widodo, and Mohd Zuki Salleh. "Numerical solution on MHD stagnation point flow in ferrofluid with Newtonian heating and thermal radiation effect." *Journal of Advanced Research in Fluid Mechanics and Thermal Sciences* 57, no. 1 (2019): 12-22.
- [31] Zaki, Abdul Muiz Mohd, Nurul Farahain Mohammad, Siti Khuzaimah Soid, Muhammad Khairul Anuar Mohamed, and Rahimah Jusoh. "Effects of heat generation/absorption on a stagnation point flow past a stretching sheet carbon nanotube water-based hybrid nanofluid with Newtonian heating." *Malaysian Journal of Applied Sciences* 6, no. 2 (2021): 34-47. <https://doi.org/10.37231/myjas.2021.6.2.297>
- [32] Rosli, Wan Muhammad Hilmi Wan, Muhammad Khairul Anuar Mohamed, Norhafizah Md Sarif, Nurul Farahain Mohammad, and Siti Khuzaimah Soid. "Blood conveying ferroparticle flow on a stagnation point over a stretching sheet: Non-Newtonian Williamson hybrid ferrofluid." *Journal of Advanced Research in Fluid Mechanics and Thermal Sciences* 97, no. 2 (2022): 175-185. <https://doi.org/10.37934/arfmts.97.2.175185>
- [33] Rosli, Wan Muhammad Hilmi Wan, Muhammad Khairul Anuar Mohamed, Norhafizah Md Sarif, and Huei Ruey Ong. "Convective Boundary Layer Flow of Williamson Hybrid Ferrofluid over a Moving Flat Plate with Viscous Dissipation." *Journal of Advanced Research in Fluid Mechanics and Thermal Sciences* 112, no. 1 (2023): 176-188. <https://doi.org/10.37934/arfmts.112.1.176188>